# ELECTRON BEAM DYNAMICS IN THE LONG-PULSE, HIGH-CURRENT DARHT-II LINEAR INDUCTION ACCELERATOR*

Carl Ekdahl, E. O. Abeyta, P. Aragon, R. Archuleta, G. Cook, D. Dalmas, K. Esquibel, R. Gallegos, R. Garnett, J. Harrison, J. Johnson, E. Jacquez, B. Trent McCuistian, N. Montoya, S. Nath, K.Nielsen, D. Oro, L. Rowton, M. Sanchez, R. Scarpetti, M. Schauer, G. Seitz, V. Smith, and R. Temple, LANL, Los Alamos, NM 87545, USA

H. Bender, W. Broste, C. Carlson, D. Frayer, D. Johnson, C. Y. Tom, C. Trainham, and J. Williams, NSTec, Los Alamos, NM 87544, USA

B. Prichard and M. Schulze, SAIC, San Diego, CA 92121, USA

T. Genoni, T. Hughes, and C. Thoma, Voss Scientific, Albuquerque, NM 87108, USA

*Abstract*

We are now operating the 74-cell DART-II linear induction accelerator (LIA) at its full energy, accelerating 2-kA electron beams to more than 17 MeV. The injector produces a beam pulse with a full-width at half maximum (FWHM) greater than 2.5 μs, with a flat-top region where the final electron kinetic energy varies by less than 1% for more than 1.5 μs. We discuss the tuning of the injector and accelerator; and present data for the resulting beam transport and dynamics. We also present beam stability measurements, which we relate to previous stability experiments at lower current and energy.

## INTRODUCTION

The Dual-Axis Radiographic Hydrotest (DARHT) facility has two linear induction accelerators (LIA) for flash radiography of explosive hydrodynamic experiments with orthogonal views. The 2-kA, 20-MeV DARHT-I LIA has been producing radiographs with a single 60-ns pulse since the year 2000. Now we are also operating the 74-cell DARHT-II LIA at 2 kA and 17 MeV. The DARHT-II LIA is unique in that its beam pulse has a long, 1.6-μs flattop during which the kinetic energy varies by les than ±1%. A kicker cleaves four short pulses out of this long pulse, and these are converted to bremsstrahlung for multi-pulse radiography.

The DARHT-II long-pulse 2-kA beam is produced in a diode powered by an 88-stage Marx generator generating a 2.5-MV output pulse at the anode-cathode (AK) gap. A diverter switch (crowbar) is incorporated to be able to shorten the 2-μs flat-top pulse to as little as 200 ns flat-top. After leaving the diode, the beam is accelerated by six induction cells to 3.1 MeV. After leaving the injector cells, the beam enters a transport zone designed to scrape off the long rise time, off-energy beam head. As in previous experiments [1,2,3], this beam-head clean-up zone (BCUZ) was configured to pass almost the entire beam head. The main LIA has 68 induction cells that accelerate the beam to more than 17 MeV. Each accelerating cell incorporates a solenoid to provide the focusing field for beam transport, as well as dipoles for beam steering.

The solenoids in the injector cells are tuned so that none of the off-energy electrons in the ~500-ns beam head are lost, even in the absence of accelerating fields. The solenoids through the main accelerator were tuned to transport a matched beam through a field increasing to more than 1 kG on axis to suppress beam breakup (BBU).

The tunes for the DARHT-II magnetic transport were designed with two envelope codes, XTR [4] and LAMDA [5]. These solve the beam-envelope differential equations keeping terms that are dropped from the usual paraxial approximation [6]. Initial conditions for XTR and LAMDA were provided by simulations of the space-charge limited diode using the TRAK gun-design code [7] and the LSP particle-in-cell code [8].

Non-invasive DARHT-II diagnostics used on every shot include diode AK potential monitored with a capacitive divider, accelerating cell potentials monitored with resistive dividers, and beam current, centroid position, and beam ellipticity measurements with 20 beam position monitors (BPM) [2,3]. Invasive diagnostics used occasionally include beam electron energy measurements with a magnetic spectrometer and beam current profile measurements using anamorphic streak imaging of Cerenkov light from fused silica targets [9].

## RESULTS

There was no loss of beam current through the LIA during the time that the accelerating cells were energized, as shown in Fig. 1, which is an overlay of beam current measurements though the injector and accelerator. For these data, the current was terminated by the crowbar, which was timed to coincide with the end of the accelerating cell pulse. The red cursors in Fig. 1 delineate the 1.6-μs flattop used for the four radiography pulses. Slight beam loss in the BCUZ during the risetime is evident. Figure 2 shows the electron kinetic energy measured with our magnetic spectrometer. The kinetic energy of the accelerated beam exceeds 17.0 MeV for more than 1.6 μs. For this measurement five of the LIA

cells were turned off, which reduced the energy by ~1.3 MeV from that expected with all 74 cells.

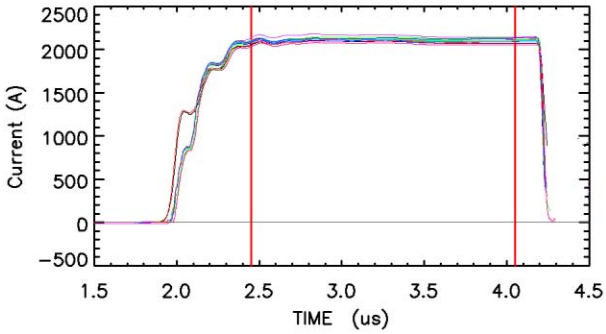


Figure 1: Overlay of beam current measurements in injector and accelerator. Red cursors indicate the 1.6-μs flattop region used for the four radiography pulses.

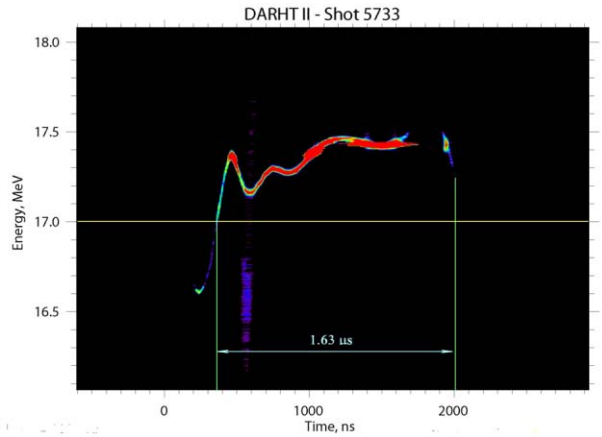


Figure 2: Magnetic spectrometer measurement of electron kinetic energy.

Low frequency beam motion at the exit of the accelerator was dominated by an energy dependent sweep resulting from random dipoles caused by small solenoid misalignments. This sweep is undesirable because it effects the locations of the four radiography pulses. Head-to-tail sweep is a characteristic of the resistive wall instability. However, in a strong solenoidal focusing field like ours this instability is independent of energy, in contradiction to our sweep data. Moreover, the predicted e-folding growth length is more than twice the length of the accelerator. The other likely cause of sweep is corkscrew, which can be suppressed using beam-steering dipoles [10]. We used steering dipoles throughout the accelerator to reduce the sweep to an amplitude acceptable for commissioning the multi-pulse radiography target. This first attempt to reduce the sweep resulted in an immediate ~40% reduction to ~3.3 mm over the 1.6-μs flat top. We anticipate further improvements by continuing to pursue our steering strategy.

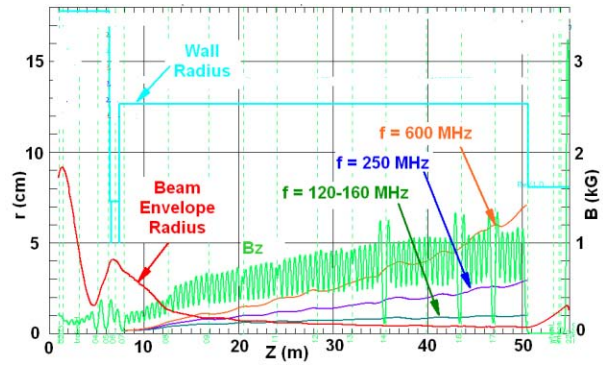


Figure 3: Beam envelope and saturated growth of BBU as calculated by XTR for our tune. The amplitude of a 50-micron initial perturbation is plotted for the three principal modes of the measured transverse impedance [12].

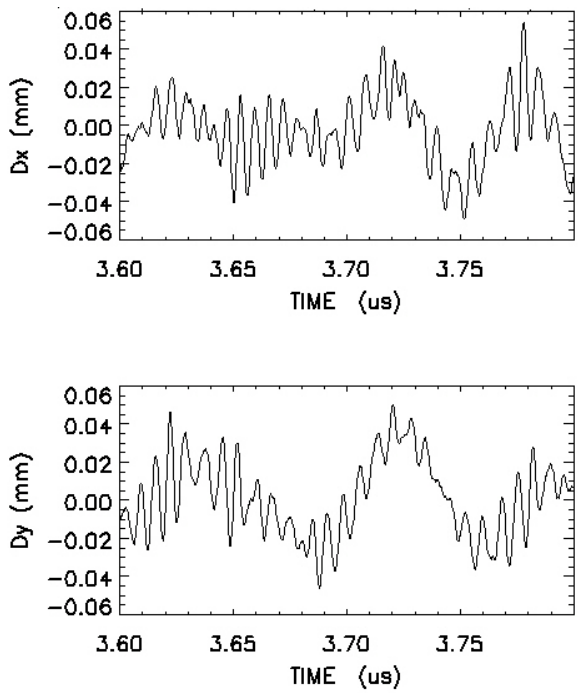


Figure 4: Beam motion at accelerator exit over 200-ns with low frequency sweep filtered out to show the BBU and a lower frequency mode thought to be ion hose..

High frequency motion at the accelerator exit was due to BBU. For the DARHT-II LIA the BBU amplitude saturates at $\xi(z)=(\gamma_0/\gamma)^{1/2}\xi_0\exp(\Gamma_m)$, where subscript zero denotes initial conditions, and $\gamma$ is the usual relativistic mass factor [3]. The maximum growth exponent is $\Gamma_m = I_b N_g Z_\perp <1/B> / 3\text{x}10^4$ [11]. Here $I_b$ is the beam current in kA, $N_g$ is the number of gaps, the transverse impedance $Z_\perp$ is in Ω/m., and the average focusing force $<1/B>$ is in $\text{kG}^{-1}$. The LIA tune had a strong enough focusing field to suppress the BBU to an acceptable amplitude (< 10% of beam radius) as shown in Fig. 3 by the expected growth

of an initial 50-micron perturbation using measured values of the transverse impedance [12].

We recorded the beam position data at the accelerator exit (BPM20) at 5 Gs/s to have enough bandwidth to resolve even the highest frequency BBU mode. Figure 4 shows the BBU amplitude at BPM20 during a 200-ns window near the end of the beam pulse. Peak amplitudes are less than 60 microns, which is about 10% of the predicted beam radius at that location.

Figure 5 shows a spectral analysis of the beam motion at the accelerator exit. In addition to the activity at the lower BBU frequencies, BBU activity at the highest frequency mode (~600 MHz) can be clearly seen. That the amplification at 600 MHz does not appear to be as strong compared with the lower frequencies (as would be expected from the transverse impedance measurements) is due to the bandwidth limitations of our BPMs and their long signal cables.

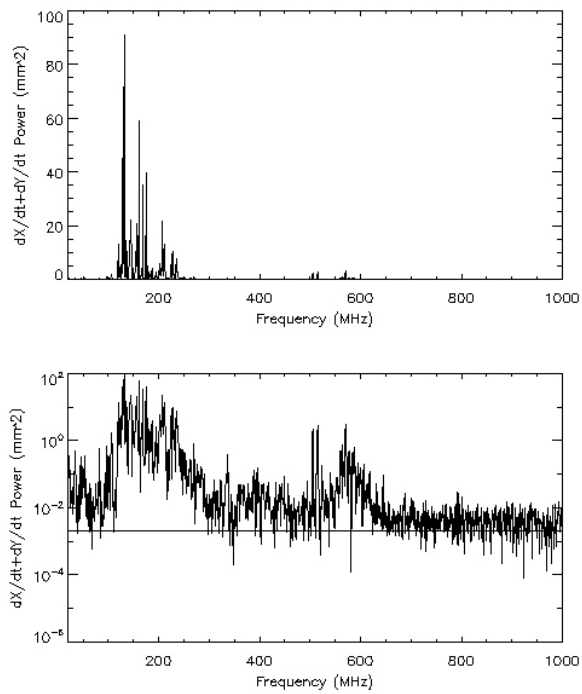


Figure 5: BBU frequency analysis of beam transverse velocity at the accelerator exit shows BBU activity in the 600-MHz band, as well as in the previously observed lower frequency bands [3].

Finally, we also observed beam motion in the 10-20 MHz range characteristic of ion hose (see Fig. 5) [3]. This could be the result of gas generated in the BCUZ.

In conclusion, we have now operated the DARHT-II accelerator at its fully rated current, energy, and pulse width. The accelerated beam was stable enough for us to proceed with commissioning the multi-pulse kicker and bremsstrahlung converter for radiography.

## REFERENCES

[1] Carl Ekdahl, et al., "First beam at DARHT-II," in Proc. 2003 Part. Accel. Conf., (2003), pp. 558-562

[2] Carl Ekdahl, et al., "Initial electron-beam results from the DARHT-II linear induction accelerator," IEEE Trans. Plasma Sci. 33, (2005), pp. 892-900.

[3] Carl Ekdahl, et al., "Long-pulse beam stability experiments on the DARHT-II linear induction accelerator," IEEE Trans. Plasma Sci. 34, (2006), pp.460-466.

[4] Thomas P. Hughes, David C. Moir and Paul W. Allison, "Beam injector and transport calculations for ITS," in Proc. 1995 Part. Accel. Conf., (1995), pp. 1207-1209

[5] Thomas .P. Hughes, et al., "LAMDA User's Manual and Reference", Voss Scientific technical report VSL-0707, April 2007

[6] E. P. Lee and R. K. Cooper, "General envelope equation for cylindrically symmetric charged-particle beams," *Part. Acc. 7*, (1976), pp. 83-95

[7] Stanley Humphries Jr., "TRAK – Charged particle tracking in electric and magnetic fields," in Computational Accelerator Physics, R. Ryne Ed., New York: American Institute of Physics, (1994), pp. 597-601 .

[8] T. P. Hughes, R. E. Clark, and S. S. Yu, "Three-dimensional calculations for a 4 kA, 3.5 MV, 2 microsecond injector with asymmetric power feed," Phys. Rev. ST Accel. Beams 2, (1999), pp. 110401-1 – 110401-6

[9] H. Bender, et al., "Quasi-anamorphic optical imaging system with tomographic reconstruction for electron beam imaging," Rev. Sci. Instrum. 78, (2007), pp. 013301

[10] J. T. Weir, J. K. Boyd, Y.-J. Chen, J. C. Clark, D. L. Lager, and A. C. Paul, "Improved ETA-II accelerator performance," in *Proc. 1999 Particle Accelerator Conf.*, New York, NY, March, 1999, pp. 3513-3515.

[11] V. K. Neil, L. S. Hall, and R. K. Cooper, "Further theoretical studies of the beam breakup instability," Particle Accelerators, vol. 9, 1979, pp. 213-222.

[12] R. Briggs and W. Waldron, "Transverse impedance measurements of the modified DARHT-2 accelerator cell design," LBNL Report #59199, November, 2005